Spatial Distribution of Droplet Diameter of Wall-Impinging-Spray for Direct Injection Gasoline Engines

Takaaki SATO　　　Naotaka SHIRABE　　　Atsuya OKAMOTO　　　Yukinobu ANEZAKI

Spray characteristics such as spray shape and spatial distribution of droplet diameter have remarkable influences on output and exhaust emissions of direct injection gasoline engines. Especially, spatial distribution of the droplet diameter after impingement of the spray against a piston cavity is one of the most important factors for output and exhaust emissions, but it is not clarified sufficiently because of the difficulties with regard to measurement. In this paper, a new laser holography method that can obtain spatial distribution of droplet diameter over the spray area in a short time was developed. And with this method, differences of spatial distribution of Sauter Mean Diameter (SMD) of droplets before and after impingement on a flat wall in a high-pressure chamber were clarified using a prototype injector. Effects of impinging angle and distance against the wall on spatial SMD distribution were also investigated.

Key words : Injector, Spray, Droplet diameter, Direct injection gasoline engine, Laser holography, Wall-impinging-spray

INTRODUCTION

A high-pressure fuel spray impinges on a piston top with the wall-guided concept that is the main stream of direct injection gasoline engines in Japan. The piston has a cavity on the top. The spray hits to the cavity and travels along the cavity wall by its momentum. Then it reaches to the spark plug and forms combustible mixture. Output and exhaust emission of the engine are affected greatly by distribution of the combustible mixture in the combustion chamber. Mixture formation is remarkably affected by the spray characteristics such as spatial distribution of the droplet diameter and fuel mass distribution and spray shape, especially after wall-impingement. Distribution of the droplet diameter after wall-impingement is one of the most important factors for mixture formation. But it is not clarified sufficiently because of the difficulties of the measurement. We aim to decide injection conditions such as injection angle and timing, pressure as well as nozzle configurations suitable for each engine efficiently by measuring spatial distribution of the droplet diameter and other characteristics after wall-impingement and clarifying the effects of injection conditions as well as nozzle configurations on them. In this paper, as its first step, a new measuring method of spatial distribution of droplet diameter over the spray in a short time was developed.

PDPA is widely adopted for measurement of droplet diameter. But the measurement area is limited and vast number of injections is required for measurement over the spray. Also, PDPA is not able to measure non-spherical droplets because it treats the signals from non-spherical droplets as noises.

The laser holography method has a potential to measure spatial distribution of droplet diameter over the spray in one injection including non-spherical droplets. Therefore, the holography method is considered as the standard measurement of droplet diameter. However, some drawbacks such as difficulty of measurement in the high-droplet-density field and long analyzing period have been major obstacles when measuring the droplet diameter over the fuel spray. Anezaki et al.[1] have solved the difficulty of measurement in the high-droplet-density by using relay lenses and a spatial filter. In this paper, authors solved the long analyzing period by constructing new software that can drive CCD camera, photographs, recognizes droplets, and analyses droplet distribution automatically. And using this method, differences of spatial SMD distribution of a prototype injector for direct injection gasoline engines between before and after wall-impingement were investigated. Effects of impinging angle and distance against the wall on spatial distribution of droplet diameter were also investigated.

PRINCIPLE OF LASER HOLOGRAPHY METHOD

The laser holography method is one of the photographic recording methods, and able to record three-dimensional information of the object. The method is classified in two, namely the off-axis and the in-line method. In the former, two laser beams are required; one is directed onto the object and called the object beam, another avoids the object and is called the reference beam. In the latter, the reference beam is combined with the object beam and only one beam is required. The in-line method has generally been used for measuring the particle diameter in the low-particle-density fields because the optical system is simple.[2][3][4] But it is difficult to obtain a clear image in the high-droplet-density fields such as the fuel spray because huge amount of droplets disturbs the reference beam. Therefore, Nishida et al.[5] used the off-axis method to measure the swirl-spray for direct injection gasoline engines. We have also used the off-axis method in order to measure the diameter in high-droplet-density fields though the optical system is more complex.

Figure 1 shows the principle of recording and reconstruction of the off-axis holography method. When recording, a laser beam is split into two; one beam is routed to illuminate the spray and the other is routed so as not to pass through the spray. Droplets in the path of the object beam diffract the beam and shift its phase. The object and the reference beam interfere with each other by crossing with each other because of the difference of their phases if the lengths of their optical paths have smaller difference than the coherent range of the laser. The interference fringes are recorded on the holographic plate placed on the cross section of two beams. A pulse laser is used to analyze high-speed objects such as high-pressure fuel spray. When reconstructing, a beam of the same quality as the reference beam, called the reconstruction beam, is incident on the holographic plate that was developed after recording. The interference fringes recorded on the plate work as diffraction gratings to convert the reconstruction beam into wave fronts of the same phase as the light passed through the spray when recording.

Then the image of the spray is reconstructed in the space. An enlarged photograph of the image is taken and a diameter of each droplet is measured. The spatial distribution of the droplet diameter is obtained by calculating the positional information of the droplets according to the focal point of the camera.
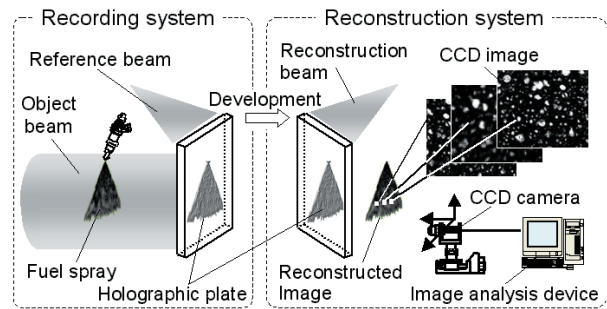

Fig. 1 Principle of holography method

EXPERIMENTAL SETUP

3.1 Laser holography

3.1.1 Recording apparatus

Figure 2 shows a recording optical system of off-axis holography applied in this study. A pulsed Nd:YAG laser (Spectra Physics, PIV200, wave length 532nm, output 200mJ) was used. An injection seeder was installed in the laser to extend the coherence range of the beams up to 2m. The laser beam was split into the object and the reference beam with a beam-splitter. Then neutral-density filters adjusted the intensity of the beams. The beams were expanded and collimated with convex lenses after their intensity distribution was homogenized with spatial filters. The object beam was directed onto the spray injected into a high-pressure chamber which provided high ambient density corresponding to particular in-cylinder condition (low engine speed, part load). A flat wall was installed in the chamber, and it was possible to measure the spray impinging on the wall. The object beam passed through relay lenses and reached to the holographic plate (Konica, P5600B, resolution 7000 lines/mm) vertically. These relay lenses made diffraction light from the droplets reach to the plate with low losses.[1][6] A pinhole was set between relay lenses with the aim of removing noises due to diffraction by dust in the air or on the optical parts from

the objective beam.[1] The reference beam bypassed the fuel spray and reached the plate with the incident angle of 45 degrees. The interference fringes due to different phase of the object and the reference beam were recorded on the plate.

Fuel was pressurized with a hand pump and an accumulator. N-heptane was used as the test fuel. The injection period and the timing of record were set freely with the delay pulse generator (Stanford Research System, DG535).
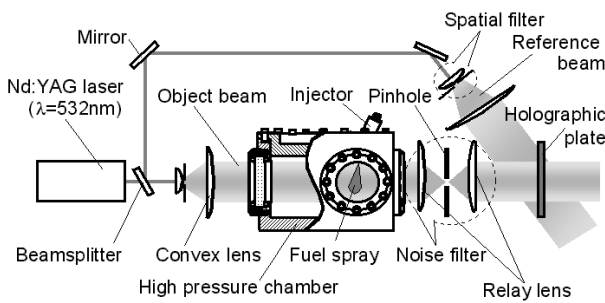

Fig. 2 Recording optical system

3.1.2 Reconstruction apparatus

The recorded holographic plate was developed, fixed, bleached, and then used for reconstruction with the optical system shown in Fig. 3. A continuous oscillation YAG laser was used in this system. A laser beam was expanded and collimated with convex lenses after the intensity distribution of it was homogenized with spatial filters. Then the beam was directed to illuminate the holographic plate from a direction of 180-degree opposite from that of recording, and the image of the spray was reconstructed. Using a CCD with a 20x objective lens attached as a microscope, enlarged photographs of the reconstructed image were taken and loaded into a personal computer. Accuracy of this laser holography
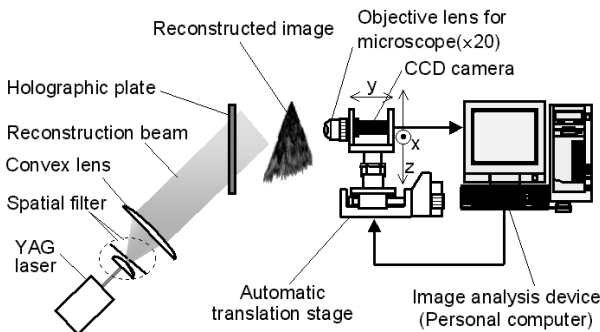
method was verified by reticles and a wire of 50 mm in the fuel spray.[1]

New software was developed that can drive CCD camera, photographs, recognizes droplets, and analyses droplet distribution automatically with the aim of reducing analysis time in this study. Figure 4 shows functions of the software. To obtain SMD distribution on the on the vertical surface (X-Z plane), the software drove the CCD camera on the X-Z plane every 1mm with an automatic pulse stage connected to a personal computer. In each point, the images of the droplets was taken and loaded to the personal computer. The spatial volume of the loaded image was $0.8 \times 0.6 \times 0.3$mm as the camera's field of view was 0.8×0.6 mm and the depth of field was 0.3 mm. The outlines of the droplets in focus were extracted and recognized by the image analysis device (Media Cybernetic, Image Pro Plus). Then, diameters of all droplets were measured and the distribution of the droplet diameter and SMD were calculated with every image. More than a few thousand images were taken when analyzing the cross section of the whole spray. In order to reduce analysis time, distribution of droplet diameter and SMD were calculated only with images in the spray. Distinction between in and out of the spray was made automatically by recognizing luminance histogram of the image. Thus spatial distributions of the droplet diameter and SMD over the entire spray were obtained in a short time automatically.
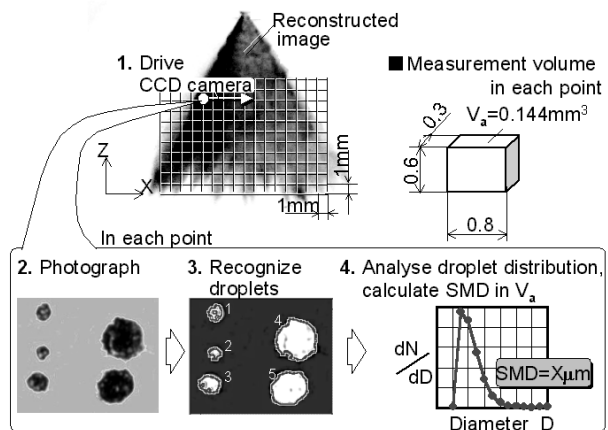

Fig. 4 Functions of analysis software

Fig. 3 Reconstruction optical system

3.2 High-speed photography

High-speed photography was applied to observe temporal images of the free spray and the wall-impinging spray. Figure 5 shows the experimental apparatus. Fuel was injected into the same high-pressure chamber that was applied to the holography system. Injection system was also the same as in the recording apparatus of the laser holography. A high-speed CCD video camera (Kodak HS4540, 9000 frame/sec) was used.
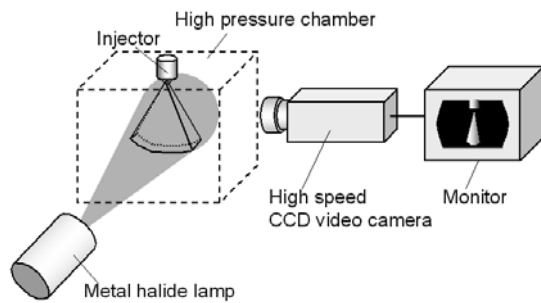

Fig. 5 Experimental apparatus for high speed photography

3.3 Experimental conditions

A prototype injector for direct injection gasoline engines is investigated.

Table 1 shows experimental conditions. A value marked with * corresponds to a particular in-cylinder condition of a real engine running at low speed, part load. Ambient density in the high-pressure chamber corresponds to the in-cylinder condition at the moment of spray-impingement on the cavity wall. Impinging angle   and distance L against the wall are defined as shown in Fig. 6.   =55 degrees and L=37mm was the base conditions, and they were changed independently to investigate the effects on spray shape and spatial distribution of droplet diameter. The difference of the impinging distance represents difference of injection timing of a real engine. Droplet distribution of the wall-impinging-spray was measured at 1ms after impingement on the wall. This timing correspond to different timing after start of injection in the case of different impinging distance L; 1.3 and 1.6ms after start of injection at L=20 and 37mm.

A free spray was also investigated and compared with the wall-impinging spray at the same timing after start of injection.

Table 1 Experimental conditions

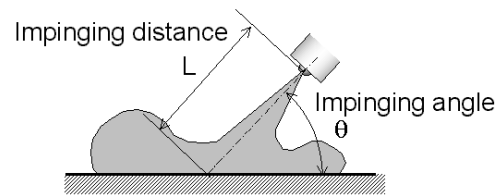| Fuel	N-heptane
Injection pressure	13 MPa*
Injection quantity	16 mm³ *
Ambient gas	Nitrogen
Ambient pressure	156 kPa.gauge
Ambient temperature	300 K
Ambient density	3.274 kg/m³ *
Impinging angle	30, 55*, 70 degrees
Impinging distance	20, 37* mm

Fig. 6 Definition of impinging angle and distance

RESULTS AND DISCUSSION

4.1 Behavior of free spray and wall-impingement spray

Comparison of shape of the free spray and the wall-impingement spray is shown in Fig. 7. The impinging distance is 37 mm and the angle is 55 degrees. Free spray increases in volume as entraining the ambient air, and becomes to be similar the gaseous jet in which eddies are shown. The shape of the wall-impinging spray is the same as that of the free spray until 0.6ms after start of injection, the timing of the wall-impingement, of course, and then, rolling-up of the spray is seen on the wall after impingement. The rolling-up moves from the impinging location to the round. Comparison of the tip penetration of the free spray and the wall-impinging spray is shown in Fig. 8. The tip penetration of the impinging spray was defined as sum of the distance from the impinging point to the tip of rolling-up and impinging distance. Compared with free spray, tip penetration of wall-impinging spray is shortened. This is because the spray increases in volume by the movement of the rolling-up to the round after wall-impingement.
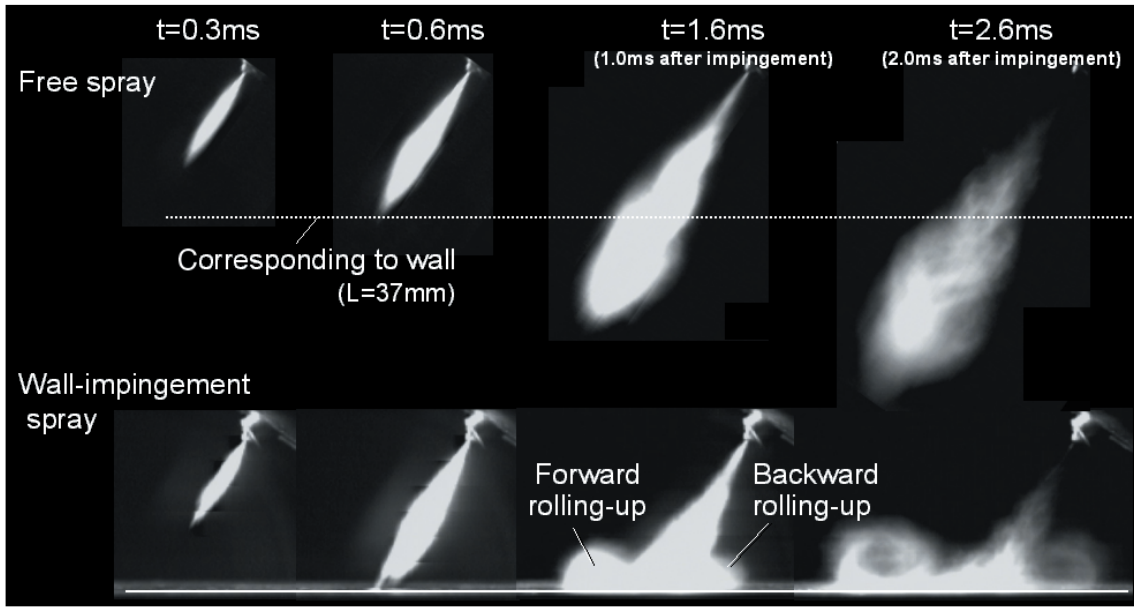
Fig. 7 Behavior of free spray and wall-impinging spray (L=37mm, =55deg.)
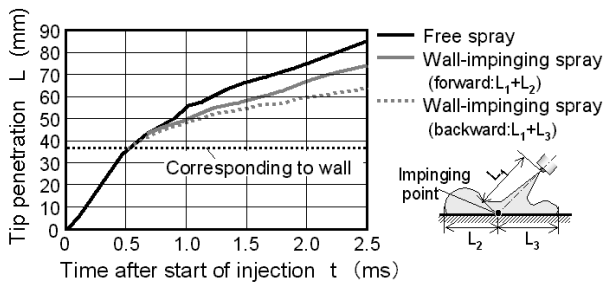

Fig. 8 Tip penetration of free spray
and wall-impinging spray

4.2 Spatial SMD distribution of free spray and wall impinging spray

Figure 9 shows the spatial SMD distribution of a free spray analyzed by the newly developed method at 0.6ms and 1.6ms after start of injection. T=0.6 ms is the timing of the wall-impingement at the base condition. SMD distribution was measured in the plane at the center of the spray as shown in this figure. These results confirm that the newly developed system can obtain spatial distribution of droplet diameter over the spray. The area colored gray indicates in which area the accurate measurement is not expected because of very high density of droplets. SMD is large at the tip of the spray at t=0.6ms, and it become larger at t=1.6ms. This is probably because smaller droplets lose their momentum early and drift around the middle of the

spray, but larger droplets keep their stronger momentum and are concentrated at the tip as the time passes.

Figure 10 shows the spatial SMD distribution of a wall-impinging spray at 1.6ms after start of injection. This is equivalent to 1.0ms after impingement. The impinging angle is 55degrees and the distance is 37mm. A larger rolling-up at the forward and smaller rolling-up at the backward can be seen respectively as the same as in Fig. 7. SMD of the area above the impinging point is almost the same as that of the free spray, but SMD of the forward rolling-up is larger compared with the area below the corresponding line to the wall shown in the free spray. In contrast, SMD of the backward rolling-up is smaller compared with the same area of the free spray. The reason may be as follows; the larger droplets penetrate forward and form the forward rolling-up by their stronger momentum, but smaller droplets lose their momentum by wall-impingement and they are blown in all directions by the gaseous jet of the spray, and they form the backward rolling-up.

Also large SMD seen at the tip of the free spray is disappeared at the wall-impinging spray. These large droplets have the possibility of being atomized by the impingement.
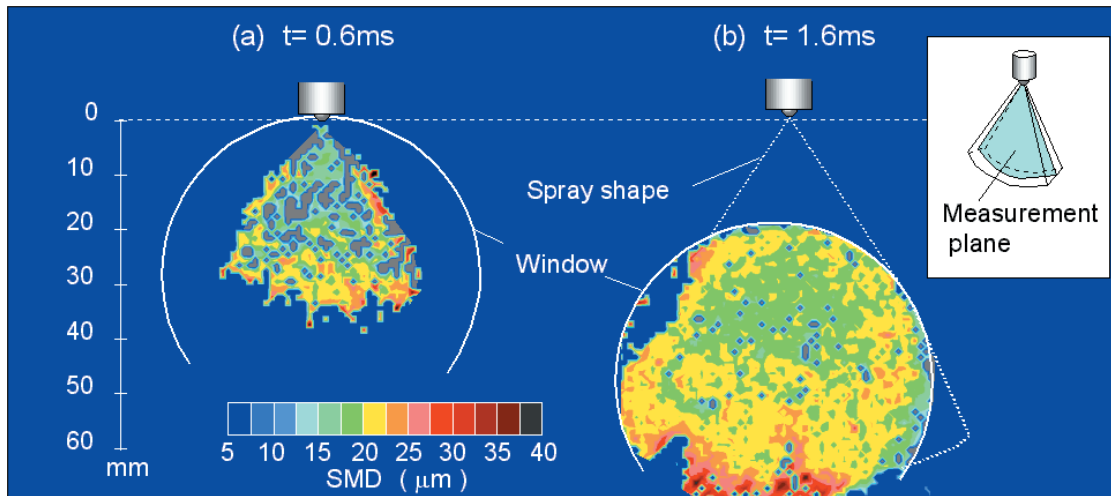
23

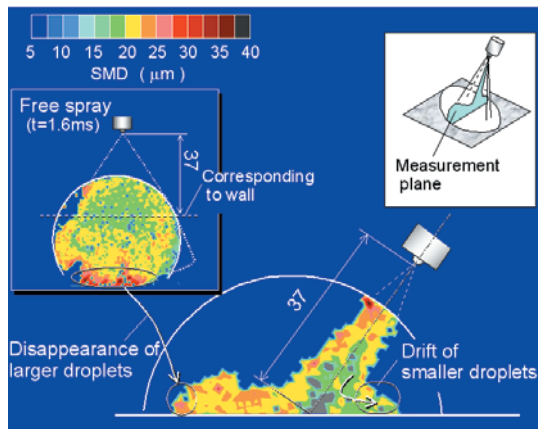Fig. 9 Spatial SMD distribution of free spray

Fig. 10 Spatial SMD distribution of wall-impinging
spray (L=37mm,　=55deg.)

4.3　Effects of impinging angle on spray
behavior and spatial SMD distribution

Effects of the impinging angle on the spray characteristics were analyzed by changing the impinging angle to the wall　from 55degrees shown before to 30, 70degrees. The impinging distance was set to 37mm.

Figure 11 shows the outline of the spray shape at 1.0ms after wall-impingement, which corresponds to 1.6ms start of injection in each case. In the case of　=70degrees, the forward rolling-up is almost the same as that of　=55degrees. But in the case of　=30degrees, the forward rolling-up is larger than those of　=55, 70degrees; the difference of the tip penetration between　=30degrees and 55degrees is 9mm, which correspond
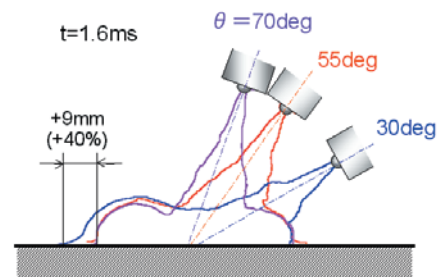

Fig. 11 Effect of impinging angle on spray shape
(L=37mm)

to 40% increase after impingement.　The reason is that in the case of　=30degrees, the spray jet impinges on the wall smoothly and keeps its momentum.

Figure 12 shows the comparison of the spray tip penetration in each case. In the case of　=70degrees, the tip penetration is shorter than that of the free spray and equivalent to that of　=55degrees.　In contrast, in the case of acute impinging angle as　=30degrees, tip penetration is equivalent to that of the free spray.
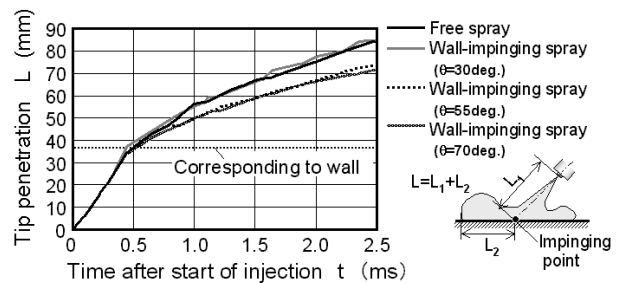

Fig. 12 Effect of impinging angle on spray tip
penetration (L=37mm)

Figure 13 shows the effects of the impinging angle on the spatial SMD distribution. In the case of the impinging angle of 70degees, the area of larger SMD in the tip of the free spray is disappeared, and there is the backward rolling-up of smaller SMD. These features are similar to those of =55degrees. In the case of =30degees, in contrast, the area of larger SMD is seen in the tip of forward rolling-up. Also there is little backward rolling-up and an area of smaller SMD can be seen near the wall in the forward rolling-up. The reason may be that smaller droplets keep their momentum through wall-impingement in the case of the smaller impinging angle, and as a result, they move to the forward rolling-up without drifting around on the wall after wall-impingement. These features are similar to those of the free spray, so the effects of wall impingement on the spray characteristics are relatively small.

4.4 Effects of impinging distance on spray behavior and spatial SMD distribution

Effects of the impinging distance on the spray characteristics were analyzed by shortening the distance to the wall L from 37mm to 20mm. The impinging angle was set to 55degrees.

Figure 14 shows the behavior of the spray in the case of L=20mm. Compared with the case of L=37mm shown in Fig. 7, the droplets forming forward rolling-up are less, and the dense cloud of droplets near the wall grow forward with their strong momentum and pierce through the forward rolling-up. Then in the case of L=20mm, compared with L=37mm, the tip penetration of the forward rolling-up is 43% longer, the height is 20% lower, and the backward rolling-up is 28% shorter as shown in Fig. 15. As a result, the droplets concentrate on the wall and mixing with the air does not progress compared with the case of the L=37mm.
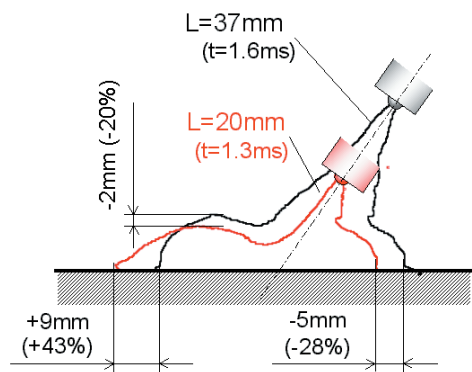

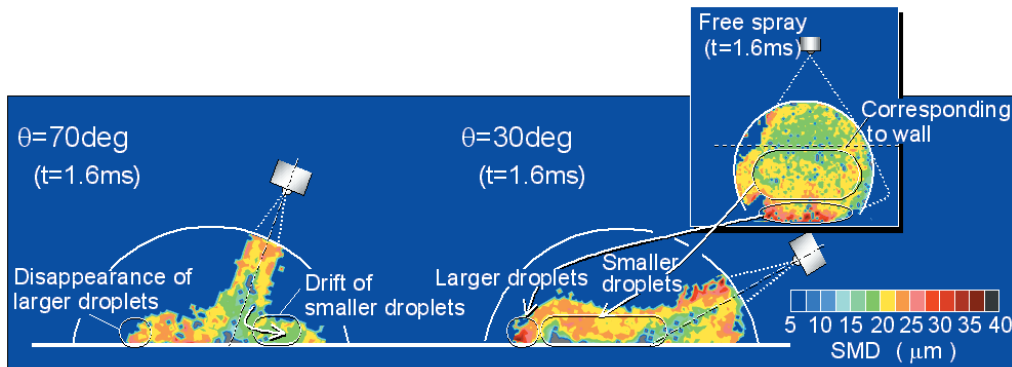Fig. 15 Effect of impinging distance on spray shape (=55deg)

Fig. 13 Effects of impinging angle on spatial SMD distribution (L=37mm)
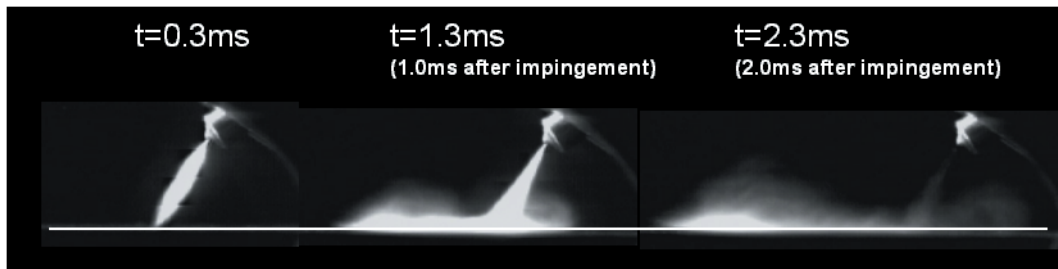

Fig. 14 Behavior of wall-impinging spray (L=20mm, =55deg)

Figure 16 shows the effects of the impinging distance on the spatial SMD distribution. The timing is 1.3ms after start of injection. SMD distribution of the free spray in this timing resembles that of t=1.6ms as shown in Fig. 9. In contrast, SMD of the wall impingement spray at L=20mm is larger than that of the free spray.

Cause of these characteristics in the case of L=20mm were considered. Figure 17 shows the spray tip penetration and the tip velocity of the free spray. The spray tip accelerates up to about 25mm of the tip penetration at these injection conditions. And then, the tip decelerates up to about 45mm of the penetration. After that, the spray loses its momentum and the velocity of the tip become obviously slower. The differences of the spray characteristics with different impinging distance can be explained by difference of the air-entrainment into the spray. Figure 18 shows the schematic diagram. The spray becomes gaseous jet as entraining the ambient air at the deceleration span from about 25mm to 45mm in the tip penetration shown in Fig. 17. The droplets are atomized into smaller ones by the shearing force with the air.[7] But at the acceleration span up to about 25mm in the tip penetration, the air is not entrained enough into the spray, so the gaseous jet does not develop enough. Also the droplets are not atomized enough into smaller ones and keep their momentum. If impinging to the wall with these conditions, the rolling-up after impingement become smaller because of the weak spray jet and the tip penetration after impingement become longer because

of the stronger momentum of the droplets. Also SMD of the impinging spray become larger compared with the free spray because breakup of the droplets into smaller ones rarely happens yet in this span. As a result, the
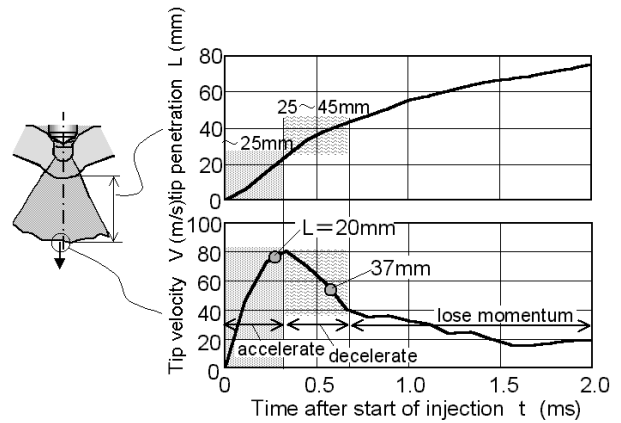

Fig. 17 Tip penetration and velocity of free spray

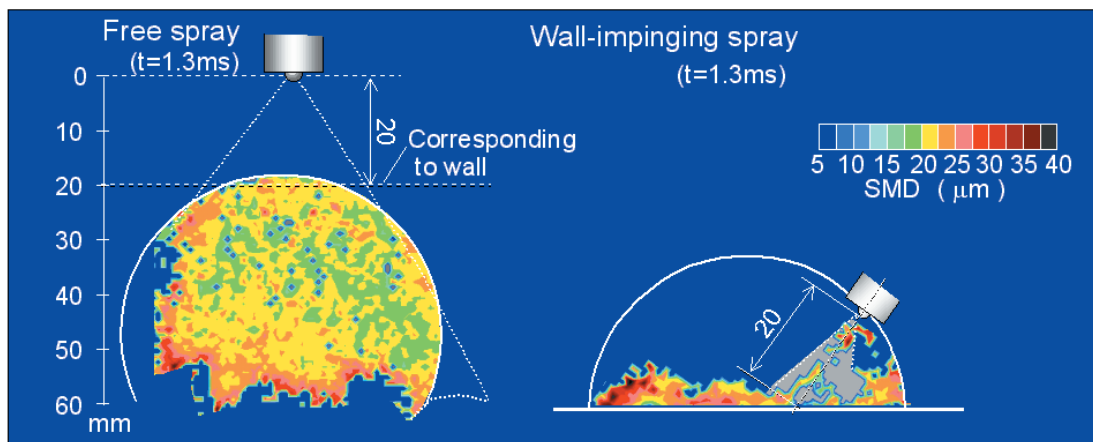Fig. 18 Cause of different spray characteristics by different impinging distance L

Fig. 16 Effects of impinging distance on spatial SMD distribution (L=20mm,   =55deg)

spray characteristics are different in the case of shorter impinging distance L as 20mm. For these reasons, it has an potential advantage for better mixing of the droplets and the air, preservation of momentum, and fine atomization to have the spray impinge against the wall in the span that the air is entrained enough into the spray and momentum of the spray is comparatively preserved.

CONCLUSIONS

1. A new laser holography method that can measure spatial distribution of SMD over the spray in a short time was developed by constructing new software that can drive CCD camera, photographs, recognizes droplets, and analyses droplet distribution automatically.

2. The newly developed method was applied for analysis of high-pressure fuel spray of a prototype injector for direct injection gasoline engines, and the following were clarified:

   a) A free spray has larger SMD in the tip, and smaller in the middle of the spray.

   b) When spray impinges on the wall, rolling-up at the forward and at the backward can be seen respectively. In the case of obtuse impinging angle, SMD of the forward rolling-up is larger and that of the backward rolling-up is smaller compared with the corresponding area of the free spray. Also the area of large SMD seen at the tip of the free spray has the possibility of being atomized by the impingement.

   c) In the case of acute impinging angle, the area of larger SMD is seen in the tip. Also there is little backward roll-up and an area of smaller SMD can be seen near the wall in the forward roll-up. These features are similar to those of the free spray, so the effects of wall impingement on the spray characteristics are relatively small in this case.

   d) In the case of shorter impinging distance L as 20mm, the droplets concentrate on the wall and mixing with the air does not progress compared with the case of the L=37mm. SMD of the wall-impinging spray in this case is larger than that of the free spray.

   e) It has an potential advantage for better mixing of the droplets and the air, preservation of momentum, and fine atomization to have the spray impinge against the wall in the span that the air is entrained enough into the spray and momentum of the spray is comparatively preserved.

ACKNOWLEDGMENTS

REFERENCES

1) Y.Anezaki, N.Shirabe, K.Kanehara, T.Sato, 3D Spray Measurement System for High Density Fields Using Laser Holography, SAE 2002-01-0739(2002)

2) M.Masuda, H.Yano, T.Aoki, K.Matsuo, Particle Sizing with Inline Laser Holography using an Ultraviolet Laser, Journal of the visualization society of Japan, Vol.18(1998), pp.71-72.

3) H.Meng, J.Estevadeordal, S.Gogineni, L.Goss, W.M.Roquemore, Holographic Flow Visualization as a tool for studying 3D Coherent Structures and Instabilities, Proceedings of The Second International Workshop on PIV'97-Fukui(1997), pp.27-34.

4) H.Meng, F.Hussain, In-Line recording and Off-axis viewing technique for holographic particle velocimetry, Applied Optics Vol.34, No.11(1995), pp.1827-1840.

5) M.Yamakawa, K.Nishida, M.Kamikawa, T.Yoshizaki, H.Hiroyasu, Development of Three Dimensional Measurement System for Droplet Size Distribution via Pulsed Laser Holography Method, Jounal of the ILASS-Japan, Vol.8, No.23(1999), pp.130-137.

6) J.Zhang, J.Katz, Off-axis HPIV with Forward Light Scattering from Particles, ASME 1994,FED-Vol.191(1994), pp.173-177.

7) R.D.Reitz, R.Diwakar, Effect of Drop Breakup on uel Sprays, SAE 860469(1986)